

Exact results for the entanglement in 1D Hubbard models with spatial constraints

Ioannis Kleftogiannis^{a,*}, Ilias Amanatidis^b, Vladislav Popkov^{c,d,e}

^a*Physics Division, National Center for Theoretical Sciences, Hsinchu 30013, Taiwan*

^b*Department of Physics, Ben-Gurion University of the Negev, Beer-Sheva 84105, Israel*

^c*Department of Physics, University of Ljubljana, Jadranska 19, SI-1000 Ljubljana, Slovenia*

^d*Department of Physics, Bergische Universität Wuppertal 42097 Wuppertal*

^e*HISKP, University of Bonn, Nussallee 14-16, 53115 Bonn, Germany*

Abstract

We investigate the entanglement in Hubbard models of hardcore bosons in $1D$, with an additional hardcore interaction on nearest neighbouring sites. We derive analytical formulas for the bipartite entanglement entropy for any number of particles and system size, whose ratio determines the system filling. At the thermodynamic limit the entropy diverges logarithmically for all fillings, except for half-filling, with the universal prefactor $1/2$ due to partial permutational invariance. We show how maximal entanglement can be achieved by controlling the interaction range between the particles and the filling which determines the empty space in the system. Our results show how entangled quantum phases can be created and controlled, by imposing spatial constraints on states formed in many-body systems of strongly interacting particles.

1. Introduction

Entanglement is a key concept in understanding how quantum orders manifest in systems with many interacting particles[1, 2, 3], such as the well known example of topological order[4, 5, 6, 7, 8, 9, 10, 11, 12]. Essentially the degree of entanglement can be used as a measure for the strength of the quantum correlations in a many-body system. In the last decades enormous advancement has been achieved in coming up with ways to quantify the quantum orders based on entanglement measures. Such well known examples are the entanglement entropy[1, 13, 14, 15] or the entanglement spectrum[8, 16, 17, 18]. These measures require splitting the system in different partitions, whose reduced density matrix can be used to calculate the entanglement entropy of each respective partition. The scaling of this entanglement entropy with the partition size, reveals important properties of the system, such as quantum criticality.[1, 13, 14, 19]

Due to the large complexity of the many-body systems under investigation, which usually contain an enormous number of particles, exact/analytical solutions of

these problems are rarely possible and difficult to obtain.

Exact methods (Bethe Ansatz and quantum inverse scattering method) are limited to the $1D$ Fermi-Hubbard model [20] and to some extent to the Bose-Hubbard model in the low-density regime [21], while approximate and numerical approaches are used to study various aspects of the Hubbard model and its extensions, see e.g. a recent review [22]. Among other extensions, a Hubbard model with additional integrability-breaking nearest-neighbor interactions was studied recently, showing an intriguing new phase of a quantum disentangled liquid [23].

In our paper we focus on purely nearest-neighbor interaction effects and derive exact/analytical results for the entanglement in $1D$ Hubbard models of hardcore bosons[15, 24, 25], with additional spatial constraints imposed by the nearest-neighbor interactions. Many-body/Fock states manifest as the ground states of these Hubbard models, as the particles organize in different spatial configurations[26]. In this paper we provide analytical solutions for the density matrix and the entanglement entropy for superpositions of such states, for any number of particles and system size. We study the bipartite entanglement and show how it varies for different system fillings. At the thermodynamic limit we find that the entropy diverges logarithmically for all fill-

*Corresponding author

Email address: ph04917@yahoo.com (Ioannis Kleftogiannis)

ings except for half-filling, with a universal prefactor $1/2$. In addition, we show how the maximal entanglement can be achieved by varying the filling. In overall, our results provide a way to tune the entanglement in Hubbard models with strong interactions, based on the empty space in the system and the interaction range between the particles.

2. Model

The states studied in this paper can be obtained by considering the ground state of a $1D$ Hubbard-like Hamiltonian with nearest-neighbor interactions [26], in the limit of large interaction U , when the hopping part can be neglected, i.e.

$$H_U = U \sum_{i=1}^{M-1} n_i n_{i+1}, \quad (1)$$

where $n_i = c_i^\dagger c_i$ is the particle number operator, with c_i^\dagger, c_i being the creation and annihilation operators for spin-less hardcore bosons on site i . The ground state of this system filled by $N < M/2$ hardcore bosons (hereafter also called particles) has a large degeneracy, since every spatial configuration of the particles respecting the hard-core restriction on sites which are nearest-neighbours (apart from the on-site hardcore restriction), has the lowest energy (see figure 1 for an illustration). We use the name NN for these states. The NN states are separated from the first excited states by an energy gap, equal to the strength of the nearest-neighbor interaction U . A superposition of all possible NN states with equal amplitudes, has the form

$$|\Psi\rangle \equiv |M, N\rangle = \frac{1}{\sqrt{d(M, N)}} \sum_P^{d(M, N)} |1010100\dots\rangle \quad (2)$$

$$d(M, N) = \binom{M - N + 1}{N}, \quad (3)$$

where $d(M, N)$ is the number of ways to distribute the N particles on M sites, assuming at least one hole between all the particles, due to the nearest-neighbor interaction. An appearance of the binomial coefficients Eq. 3 in the sum Eq. 2 signalizes a presence of permutation group symmetry in the problem. Quantifying the impact of the hardcore constraint on nearest-neighbor sites (spatial constraint) on the entanglement entropy of a block is one of our objectives.

Note that the states of type Eq. (2) also arise in Hubbard models with dynamic restrictions not allowing cluster formation of the particles. For example,

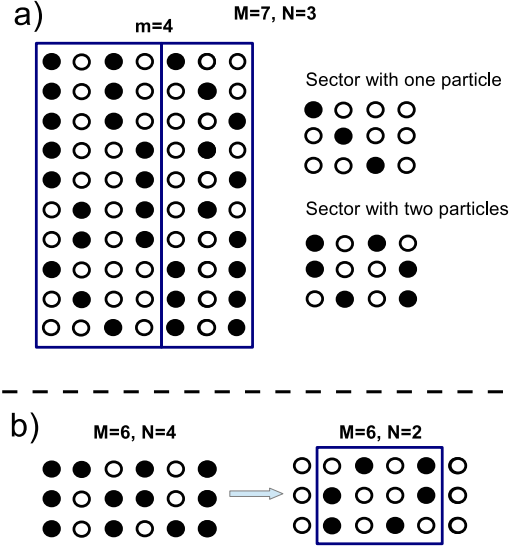


Figure 1: a) The possible NN states with nearest-neighbor interaction for $N = 3$ particles distributed in $M = 7$ sites corresponding to filling $f = 3/7$. The reduced density matrix of a partition containing $m=4$ sites, can be written in a block diagonal form. Each block corresponds to a sector according to the number of particles it contains, as shown on the right. b) NN states with $N = 4$ and $M = 6$ for filling $f > 1/2$. By applying particle-hole exchange, the NN states transform to those corresponding to a system with $N = 2$ and $M = 6$, for $f < 1/2$. This way, by ignoring the two empty edge sites we can calculate the entanglement entropy for $f > 1/2$ by knowing the one for $f < 1/2$.

the unique groundstate of the following Hubbard-like Hamiltonian

$$H = U \sum_{i=1}^{M-1} n_i n_{i+1} + t \sum_{i=1}^{M-1} [(1 - n_{i-1}) c_i^\dagger c_{i+1} (1 - n_{i+2}) + h.c.], \quad (4)$$

with $U > 0, t > 0$ contains contribution from all the NN states with different amplitudes, while at the limit $t \rightarrow 0$, the state (2) becomes one of degenerate groundstates of (4).

3. Bipartite entanglement

In this section we derive analytical results for the reduced density matrix and the entanglement entropy for partitioned superpositions of the NN states described by Eq. 2.

Due to partial permutational symmetry enjoyed by the global pure state of the system, the eigenvalues of

the reduced density matrix can be obtained after splitting the system of size M in two parts containing m and $M - m$ sites respectively, and tracing out the degrees of freedom of the m sites. The tracing out procedure can be characterized via a permutation group analysis.

As a result of the analysis, the number of non-zero eigenvalues of the reduced density matrix grows not exponentially, but linearly with the subsystem size m . Origin of all the nonzero eigenvalues have been identified, as belonging to sectors with different symmetry and particle number and it was understood how to obtain them analytically, via a recursion procedure. An example of this procedure is shown schematically in figure 1(a) for a small system. The full analytic answer has been obtained for arbitrary N, M . Also, the respective thermodynamic limit has been analyzed.

After tracing out the m sites, and using recurrently a well known formula

$$\binom{F+1}{N} = \binom{F}{N-1} + \binom{F}{N}, \quad (5)$$

after some algebra we obtain that the reduced density matrix is split into blocks

$$\rho_{M-m} = \sum_{k=0}^{m/2} A_{k0} |0_k\rangle \langle 0_k| + A_{k1} |1_k\rangle \langle 1_k| \quad (6)$$

$$|0_k\rangle = |M-m, N-k\rangle \quad (7)$$

$$|1_k\rangle = |M-m-1, N-k\rangle \otimes |1, 0\rangle \quad (8)$$

$$A_{k0} d(M, N) = \binom{m-k}{k} \binom{M-N+1-m+k}{N-k} \quad (9)$$

$$A_{k1} d(M, N) = \binom{m-k}{k-1} \binom{M-N-m+k}{N-k} \quad (10)$$

$$\langle 1_k | 1_k \rangle = \langle 0_k | 0_k \rangle = 1. \quad (11)$$

Note that the property $\text{Tr} \rho_{M-m} = 1$ is guaranteed by

$$\sum_{k=0}^{m/2} (A_{k0} + A_{k1}) = d(M, N). \quad (12)$$

Now, the states $|0_k\rangle, |\alpha_{k'}\rangle$ are orthogonal for $k \neq k'$ but they are not orthogonal for $k' = k$. The overlap between $|0_k\rangle, |1_k\rangle$ can readily be found from the combinatorial arguments to be

$$\eta_k = \langle 0_k | 1_k \rangle = \sqrt{\frac{\binom{M-N-m+k}{N-k}}{\binom{M-N+1-m+k}{N-k}}}. \quad (13)$$

Each block with $N-k$ particles thus contains two eigenvalues λ_k, μ_k , which can be found by diagonalizing the 2×2 block in (6). It is then straightforward to obtain the relations

$$\lambda_k + \mu_k = A_{k0} + A_{k1} = b \quad (14)$$

$$\lambda_k \mu_k = A_{k0} A_{k1} (1 - \eta_k^2) = c. \quad (15)$$

In terms of the above notations we have

$$\lambda_k = \frac{b}{2} + \frac{1}{2} \sqrt{b^2 - 4c} \quad (16)$$

$$\mu_k = \frac{b}{2} - \frac{1}{2} \sqrt{b^2 - 4c}. \quad (17)$$

The set λ_k and μ_k for all $0 \leq k \leq m/2$ gives the exact spectrum of the reduced density matrix for arbitrary system parameters.

3.1. Thermodynamic limit

First, consider the limit

$$N \gg m \gg 1, \quad N/M = f < 1/2. \quad (18)$$

In this limit, analogically to [13], and denoting

$$p = \frac{f}{1-f} \quad (19)$$

$$q = 1-p = \frac{1-2f}{1-f} \quad (20)$$

$$n = m-k \quad (21)$$

we obtain

$$A_{k0} \approx \frac{1}{\sqrt{2\pi npq}} e^{-\frac{(k-np)^2}{2npq}} \quad (22)$$

$$A_{k1} \approx \frac{1}{\sqrt{2\pi npq}} e^{-\frac{(k-1-np)^2}{2npq}} \frac{N-k+1}{N-M+1-n} \quad (23)$$

valid for $npq \gg 1$. After some algebra, denoting

$$x = \frac{1-k/m}{1-f} \quad (24)$$

we obtain

$$A_{k0} \equiv A_{k0}(x) = (1-f) \frac{1}{m(1-f)} g(A, x) \quad (25)$$

$$A_{k1} \equiv A_{k1}(x) = f \frac{1}{m(1-f)} g\left(A, x - \frac{\kappa(f)}{m}\right) \quad (26)$$

$$g(A, x) = \sqrt{\frac{A}{x\pi}} e^{-A \frac{(x-1)^2}{x}} \quad (27)$$

$$\int_0^\infty g(A, x) dx = 1 \quad (28)$$

$$\sum_k \dots \approx m(1-f) \int_0^\infty \dots dx \quad (29)$$

$$A = m \frac{M}{M-m} \frac{1-f}{2f(1-2f)}. \quad (30)$$

Note that the last formula is valid for comparable $M \gg 1$, $m \gg 1$, $m/M = \text{const}$, and $\kappa(f)$ is of order 1. Finally, in the zero non-vanishing order of $1/m$, the term $\kappa(f)/m \ll 1$ in Eq. 26 can be neglected, and we obtain the final formula for the eigenvalues of the reduced density matrix (RDM) of the form

$$\lambda_k \equiv \lambda(x) = \frac{C_0}{m(1-f)} g(A, x) \quad (31)$$

$$\mu_k \equiv \mu(x) = \frac{C_1}{m(1-f)} g(A, x) \quad (32)$$

$$C_0, C_1 = \frac{1}{2} \pm \frac{\sqrt{1-4f^2}}{2}. \quad (33)$$

It can be proved easily that

$$m(1-f) \int_0^\infty (\lambda(x) + \mu(x)) dx = 1. \quad (34)$$

Finally, we can find the von Neumann entropy (VNE) of the RDM, $S = -\text{tr} \rho \log \rho$, ρ being the reduced density matrix

$$S(f, m, M) = - \sum_k (\lambda_k \log \lambda_k + \mu_k \log \mu_k) \approx -m(1-f) \int_0^\infty (\lambda(x) \log \lambda(x) + \mu(x) \log \mu(x)) dx. \quad (35)$$

Performing the calculations, we obtain

$$S(f, m, M) = Q_0\left(\frac{m}{M}, f\right) + \frac{1}{2} \log m \quad (37)$$

$$Q_0 = - \sum_{\alpha=0,1} C_\alpha \log C_\alpha + \log \frac{(1-f)\sqrt{\pi e}}{\sqrt{A/m}}. \quad (38)$$

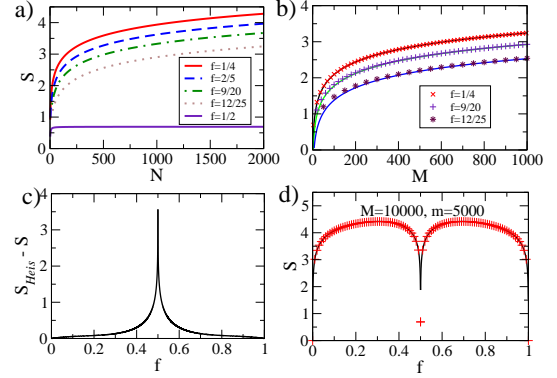


Figure 2: a) The scaling of the bipartite entanglement entropy S with the number of particles N , for different fillings. A logarithmic divergence at the thermodynamic limit can be observed in all cases, apart for the half-filled case $f = 1/2$. b) Scaling of von Neumann entropy S with the system size M . An excellent agreement can be seen between the exact results (points) obtained by Eq. 16-17 and the curves obtained in the thermodynamic limit via Eq. 37-38. c) Comparison with the entanglement entropy of a Heisenberg spin chain. The difference between the entropies of the respective systems is plotted versus the filling using Eq. 39 and a symmetry property $S(f) = S(1-f)$ established in sec. 3.2. d) The entropy versus f for a chain with $M = 10000$ and $m = 5000$ using Eq. 38. Maximum entanglement is obtained at $f \simeq 0.305$ and $f \simeq 0.695$. For $f = 1/2$ minimum entanglement with $S = \log(2)$ is achieved. An excellent agreement can be seen between the exact results (points) and the thermodynamic limit approximation (curve).

Thus we have the same logarithmic growth of the entanglement entropy of Von Neumann, $\frac{1}{2} \log m$ as in fully permutational states of the Heisenberg ferromagnet at isotropic point, see [13, 27], which is apparently due to partial underlying permutational symmetry of the initial pure state. The prefactor $1/2$ in $\frac{1}{2} \log m$ is thus simply the value of effective local spin as discussed in [27]. A comparison between the exact results of Eq. 16-17 and the thermodynamic limit Eq. 37-38 is shown on figure 2b.

Note that in the form (38) an arbitrary base of logarithm can be considered. In particular, comparing (38) with the VNE computed for the ground state of the isotropic Heisenberg ferromagnet, denoted below as S_{Heis} , see [13], we obtain

$$S_{Heis} - S = \sum_{\alpha=0,1} C_\alpha \log C_\alpha - \frac{1}{2} \log(1-2f). \quad (39)$$

As further analysis shows, $S_{Heis} > S$ for all nonzero fillings f . This has the following interpretation: the ground state of the isotropic Heisenberg ferromagnet is fully permutational invariant state with no constraints except the hard-core constraint: the minimal distance

between two particles is equal to 1: two particles can be at neighbouring sites. The wave function Eq. 2 has an additional constraint of a minimal distance between particles being equal to 2. This additional constraint lowers the symmetry of the problem, and respectively the entanglement becomes smaller. The difference $S_{Heis} - S$, shown in figure 2c, quantifies this excess of entanglement in a state with full permutational symmetry. The difference $S_{Heis} - S$ increases with the filling f , reaching a maximum at $f = 1/2$, since the effect of the additional constraint with increasing number of particles $fM = N$ becomes more and more pronounced.

Our approach of controlling the entanglement via spatial constraints in hardcore bosonic systems, could be applied also to other systems that obey similar rules. One example would be spinless fermions on a chain, since also in this case only one particle is the maximum occupation number per site. The corresponding state described by Eq. 2 should contain Fock states which are antisymmetric under exchange of two fermions, this being one of the differences with hard-core bosons, which obey the symmetry principle instead. Nevertheless, similar entanglement properties should be observed to the hardcore bosonic system, as long as the fermionic system lies in the strong interaction regime, where the fermions behave as localized(point) particles. In general, the entanglement properties of the ground state are fully determined by the microstructure inside the Fock states in equation 2 along with their superposition amplitudes, irrespectively of the type of particles.

3.2. Entanglement for $f > 1/2$

The analysis we presented so far is valid for fillings $f < 1/2$, as we have considered a wavefunction of the form Eq. 2, which has at least one hole/empty site between all the particles (minimal distance 2 between the particles). This analysis can be easily generalized to the states for $f > 1/2$ which will contain clusters of particles and a fixed number of particle pairs. These $f > 1/2$ states can be transformed to states with $N \rightarrow M - N$ and $M \rightarrow M - 2$, i.e. to those with $f < 1/2$. This can be seen by taking the states for $f > 1/2$ (note that all configurations for $f > 1/2$ have edge sites filled), exchanging particles with holes and tracing out the edge sites 1 and M , see figure 1b for an example. Therefore, the system of M sites, N particles, corresponding to $f = N/M > 1/2$ is mapped onto a system of $M' = M - 2$ sites, $N' = M - N$ particles, with filling factor $f' = (M - N)/(M - 2) \leq 1/2$. Note that for odd system size M and $N = (M + 1)/2$, only one NN state $|1010 \dots 101\rangle$ contributes to the superposition Eq.

2, leading to $S = 0$ for all m . The eigenvalues of the reduced density matrix for $f = N/M > 1/2$ are given by substituting $M \rightarrow M - 2$ and $N \rightarrow M - N$ in Eq. 16-17. In the thermodynamic limit, the configurations with fillings $f > 1/2$ are mapped onto configurations with fillings $f' = 1 - f$, leading to logarithmic behavior of the entropy for all $f \neq 1/2$.

3.3. Entanglement control

Another point of interest is the dependence of the entanglement strength on the filling. In figure 2d, we plot S versus the filling using Eq. 38(curve) and compare with the exact result using Eq. 16-17(points). The case M odd and $N = (M + 1)/2$ which gives $S=0$, is not present in figure 2d, since the system size M is even. The entropy is symmetric around $f = 1/2$ where $S = \log(2)$, due to the $f \rightarrow 1 - f$ symmetry, as we have analyzed in the previous section. The entropy obtains a maximum value at $f \simeq 0.305$ and $f \simeq 0.695$ leading to a maximally entangled quantum phase, irrespectively of the partitioning as long as both fm, fM are large (the asymptotic value $f \simeq 0.305884$ is obtained in the limit $m, M \rightarrow \infty$). The maximization of the entropy at this filling is a consequence of the spatial restrictions due to the nearest-neighbor interaction, that impose the constraint of a minimal distance 2 between the particles. Changing this minimal distance by controlling the interaction range, for example by adding a second nearest instead of nearest-neighbor interaction term in the Hamiltonian, will lead to different fillings where the maximum entanglement occurs. Consequently the entanglement strength in superpositions of states like the NN ones considered in the paper, can be tuned by the system's filling and the range of interaction between the particles.

4. Summary and Conclusions

We have studied analytically the entanglement properties of NN states, which appear as the ground states of Hubbard chains of hardcore bosons, with strong nearest-neighbor interactions i.e. 1D Hubbard models with spatial constraints. We have derived exact expressions for the entanglement entropy and the reduced density matrix for partitioned superpositions of the NN states. We have done that for any number of particles and system size, whose ratio determines the system filling.

We show that the bipartite entanglement entropy diverges logarithmically for all fillings, apart from half-filling, as in the critical phases of XY spin chains. We present a detailed analysis of the mechanism that creates the entanglement and make a comparison with the

entanglement of spin chains. The entanglement entropy obtains a maximum value for specific fillings, revealing a maximally entangled quantum phase. In overall, the conditions under which this phase occurs are determined by the spatial restrictions imposed by the empty space in the system and interaction range between the particles.

In conclusion, we show analytically how the entanglement can be tuned in Hubbard models with strong nearest-neighbor interactions, by controlling the empty space in the system and the nature of the interactions between the particles, which impose spatial restrictions on their self-organization. We hope that our results motivate further investigations on the mechanisms that allow controllable entanglement in many-body systems, to reveal novel quantum phases of matter and help with their potential application in the rapidly evolving field of quantum information technology.

Acknowledgements

IK acknowledges resources and financial support provided by the National Center for Theoretical Sciences of R.O.C. Taiwan. IA acknowledges support from the Center for Theoretical Physics of Complex Systems in Daejeon Korea under the project IBS-R024-D1. VP acknowledges financial support from Deutsche Forschungsgemeinschaft through DFG projects KO 4771/3-1 and KL 645/20-1 and support from ERC grant 694544 OMNES, and thanks Center for Theoretical Physics of Complex Systems in Daejeon Korea for a hospitality during his stay, during which this project has initiated.

References

- [1] Vidal G, Latorre J I, E. Rico and Kitaev A 2003 Phys. Rev. Lett. **90** 227902
- [2] Amico L, Fazio R, Osterloh A and Vedral V 2008 Rev. Mod. Phys. **80** 517
- [3] Horodecki R, Horodecki P, Horodecki M and Horodecki K 2009 Rev. Mod. Phys. **81** 865
- [4] Chen X, Gu Z-C and Wen X-G 2010 Phys. Rev. B **82** 155138.
- [5] Kitaev A and Preskill J 2006 Phys. Rev. Lett. **96** 110404
- [6] Kitaev A Y 2003 Ann. Phys. (NY) **303**
- [7] Levin M and Wen X-G 2006 Phys. Rev. Lett. **96** 110405
- [8] Li H and Haldane F D M 2008 Phys. Rev. Lett. **101** 010504
- [9] Haldane F D M 1983a Phys. Lett. A **93** 464
- [10] Christopher N V, Sun K, Rigol M and Galitski V 2010 Phys. Rev. B **82**, 115125
- [11] Isakov S V, Hastings M B and Melko R G 2011 Nature Physics volume **7**, pages 772-775
- [12] Affleck I, Kennedy T, Lieb E H and Tasaki H 1987 Phys. Rev. Lett. **59**, 799
- [13] Popkov V and Salerno M 2005 Phys. Rev. A **71**, 012301
- [14] Hama A Ionicioiu R and Zanardi P 2005 Phys. Rev. A **71**, 022315
- [15] Wang Y, Gulden T and Kamenev A 2016 Phys. Rev. B **95**, 075401
- [16] Alba V, Haque M and Luchli A M 2013 Phys. Rev. Lett. **110**, 260403
- [17] Calabrese P and Lefevre A 2008 Phys. Rev. A **78**, 032329
- [18] Pollmann F, Turner A M, Berg E and Oshikawa M 2010 Phys. Rev. B **81**, 064439
- [19] Eisert J, Cramer M and Plenio M B 2010 Rev. Mod. Phys. **82**, 277
- [20] F. H. L. Essler, H. Frahm, F. Göhmann, A. Klümper, V. E. Korepin, The one-dimensional Hubbard model (Cambridge University Press, Cambridge, UK, 2005)
- [21] Krauth W 1991 Phys. Rev. B **44**, 9772
- [22] Carmelo J M P and Sacramento P D 2018 Physics Reports **749** 1
- [23] Garrison J R, Mishmash R V, Fisher Matthew P A 2017 Phys. Rev. B **95**, 054204
- [24] Hen I and Rigol M 2009 Phys. Rev. B **80**, 134508
- [25] Nishimoto S, Ejima S and Fehske H 2013 Phys. Rev. B **87**, 045116
- [26] Kleftogiannis I, Amanatidis I 2017 arXiv:1707.07840
- [27] Popkov V, Salerno M and Schütz G M 2005 Phys. Rev. E **72**, 032327